Cerium Modified Nanocrystalline SmFeO$_3$ for Ethanol Sensing

R. B. MANKAR[1*] and V. D. KAPSE[2]

[1*]Department of Physics, Smt. Radhabai Sarda Arts, Commerce and Science College, Anjangaon Surji 444705, Maharashtra State, India.
[2]Department of Physics, Arts, Science and Commerce College, Chikhaldara 444807, Maharashtra State, India.
*Corresponding author E-mail: rbmankar@gmail.com

ABSTRACT

Presently, detection of ethanol has become essential in various fields due to its adverse effects on human beings. For selective detection of ethanol, chemiresistive gas sensors are widely investigated. Modified ABO$_3$ type perovskites have shown their potential in the fabrication of chemiresistive gas sensors. In present work, SmFeO$_3$ perovskite oxide based thick films were fabricated and surface modified with cerium by simple dipping technique. The structural properties of the samples were studied by Field Emission Scanning Electron Microscopy (FE-SEM) and Energy Dispersive X-ray spectrometer (EDS). The results of FE-SEM indicate that average grain size was in nano range and Ce-modified SmFeO$_3$ films were comparatively more porous than pure SmFeO$_3$ film. This porous nature of film favors gas sensing mechanism. The results of EDS suggest that Ce was deposited on the surface of SmFeO$_3$ films. The gas response of pure SmFeO$_3$ film was tested towards LPG, CO$_2$, NH$_3$, H$_2$, C$_2$H$_5$OH, Cl$_2$, and H$_2$S gases and observed that SmFeO$_3$ film exhibited good response to ethanol (C$_2$H$_5$OH). Among modified samples, Ce-modified SmFeO$_3$ film (dipping time 5 min) exhibited excellent ethanol sensing properties such as, maximum response (16.87 at 100^{0}C), response time (24 sec), recovery time (34 sec), excellent stability, and good selectivity towards ethanol. Thus Ce-modified SmFeO$_3$ is a potential material in the fabrication of ethanol sensor. The impacts of Ce modification on the gas sensing performance of the SmFeO$_3$ sensor ware discussed in detail.

Keywords: Gas response, SMO gas sensor, SmFeO$_3$, Surface modification, Sol-gel method.

INTRODUCTION

Development of gas sensors for environmental monitoring has been an active area of research. Among various gas sensors, chemiresistive gas sensors have proved their potential in the detection of hazardous gases. Metal oxide semiconductors have been extensively studied as promising material for selective detection of gases[1-2]. So far, n-type metal oxides semiconductors like ZnO, TiO$_2$, SnO$_2$, LaFeO$_3$, and WO$_3$ were frequently reported for chemiresistive gas sensors[3-7]. They have high sensitivity, low cost and their sensing mechanism is well explained. On the other hand, p-type semiconductors have been relatively less explored for chemiresistive gas sensors. Exploitation of their interactions with target gas may lead to new sensors with enhanced properties.

$SmFeO_3$ is p-type metal oxide semiconductor usually studied as a chemiresistive gas sensor material for the detection of oxidizing gases[8-11]. It has an orthoferrite phase and ABO_3-type perovskite oxide structure[8]. Its resistance decreases in presence of ozone, oxygen, NO_2, etc. and increases with exposure to reducing gases like ethanol, ammonia, etc. At low temperature, electrical conductivity of $SmFeO_3$ is very small for both oxidizing and reducing gases which results in lack of response. Moreover, $SmFeO_3$ is not stable due to the phase separation of Sm_2O_3 when exposed to reducing gases[12-13]. Due to these two reasons, the applicability of $SmFeO_3$ is limited to detection of oxidizing gases at higher temperature. Now, chemical stability and electric conductivity are related with cations at A and B sites in ABO_3 type perovskite oxide. Therefore doping of $SmFeO_3$ could be an effective approach not only to increase its electrical conductivity but also to use it under reducing conditions. Doping Co, Ni or Mg in $SmFeO_3$ have been attempted to increase electrical conductivity of $SmFeO_3$. But still there is a problem of stability in reduction conduction with these dopants since, Co-O, Ni-O and Mg-O bonds are weaker.

Ethanol is one of the most volatile and flammable gas[14]. It is used in sanitizer, chemical industries and in industrial production. Different organs of the body including the brain can have serious some time permanent damage due to heavy ethanol drinking[15-16]. Therefore, ethanol-monitoring is strongly required. $SmFeO_3$ was reported for ethanol gas detection but optimal operating temperature was very high around 370^0C[17-18]. To reduce the optimal operating temperature, Ma Zhao et al. prepared Co-doped $SmFeO_3$ and obtained maximum response to 300 ppm ethanol at lower optimal operating temperature 215^0C[19]. Cobalt doping improved electrical conductivity of $SmFeO_3$ but reduced the chemical stability in the reducing environment. S. M. Bukhari *et al.,* investigated that Ce doping in $SmFeO_3$ improved the electrical conductivity and also prevent it from decomposing under a reducing environment[12]. Thus Ce-doped $SmFeO_3$ based gas sensor can be employed for detection of reducing gases like ethanol.

To the best of our knowledge, optimal operating temperature for doped $SmFeO_3$ based ethanol gas sensor was above 200^0C and only volume doping was investigated. Therefore in present work, attempt was made to modify $SmFeO_3$ thick films by surface doping with cerium chloride using dipping method. The effect of Ce surface modification on ethanol gas sensing properties of $SmFeO_3$ based gas sensor was investigated. The results depicted that Ce-modified $SmFeO_3$ thick film with dipping time interval 5 min exhibited excellent ethanol response at reduced optimal operating temperature 100^0C.

MATERIAL AND METHODS

Fabrication of Thick Films

Pure $SmFeO_3$ powder was prepared by sol-gel method briefly described in our earlier publication[20]. The screen printing method was reported by many authors to fabricate thick films of semiconducting metal oxides[21-23]. Thixotropic paste was prepared from the mixture of the fine powder of $SmFeO_3$ and organic vehicles. This thixotropic paste was then deposited over the glass substrates by using a squeegee. After drying in air, the films were fired at 500^0C for half an hour in Muffle Furnace.

Surface Modification of Thick Films

For surface modification, the dipping technique was adopted as reported by some researchers[24]. 0.1 M aqueous solution of cerium chloride was prepared and to this solution $SmFeO_3$ thick films were dipped. The dipping time intervals were 1 min, 3 min, and 5 minute. These films are now identified as "Ce-surface modified $SmFeO_3$ thick films". They were dried in air for 48 h before their firing in Muffle Furnace at 550^0C.

XRD spectrum of $SmFeO_3$ powder was studied to confirm its structure. To observe microstructure and compositions of the films, their FE-SEM with EDS spectra were recorded.

For examining the sensing properties of as prepared thick films, static gas sensing set-up was used which essentially consists of heater mounted on base plate and glass dome. Using silver electrodes, electrical contacts were made with thick film. During the experiment,

the operating temperature was adjusted from room temperature to 400°C. Target gas of fixed concentration (60 ppm) was inserted inside the dome through gas inlet valve using syringe. In the test process, constant voltage was applied to the sensor and the current was measured using digital pico-ammeter in presence of air and the target gases. The gas response is determined from the relation

$$S = \frac{R_g}{R_a}$$ (1)

Where, 'R_a' denotes sensor resistance in air and 'R_g' denotes its resistance in target gas at the same temperature[14]. The selectivity of the film is tested against H_2S, LPG, NH_3 CO_2, C_2H_5OH, Cl_2, and H_2.

RESULTS AND DISCUSSION

X-Ray Diffraction Study

XRD spectrum of pure $SmFeO_3$ powder was presented and discussed in detail in our earlier publication[20]. The well defined sharp peaks of high intensity were obtained at 22.94°, 25.65°, 31.97°, 32.71°, 33.16°, 46.73°, 53.26°, 58.91°, 68.54°, and 78.31°. The corresponding lattice planes were respectively (101), (111), (200), (121), (002), (202), (311), (042), (242), and (421). The results well matches with the standard JCPDS card number 39-1490 and confirmed the perovskite phase with orthorhombic symmetry and Pnma space group. The average crystallite size was calculated using Scherrer's formula

$$d = \frac{0.9\lambda}{\beta cos\theta}$$ (2)

Where 'λ' is wavelength of X-ray, 'θ' is diffraction angle and 'β' is Full Width at Half Maximum (FWHM). The average crystallite size was estimated as d=50.08 nm. The values of lattice parameters 'a', 'b' and 'c' were 5.604 Å, 7.704 Å, and 5.397 Å respectively. The unit cell volume is calculated to be V=233.05 Å³.

Morphological Analysis

Fig. 1 (A) is the FE-SEM image of pure $SmFeO_3$. Fig. 1 (B-D) are the FE-SEM images of Ce-surface modified $SmFeO_3$ with dipping time intervals 1 min, 3 min and 5 minute.
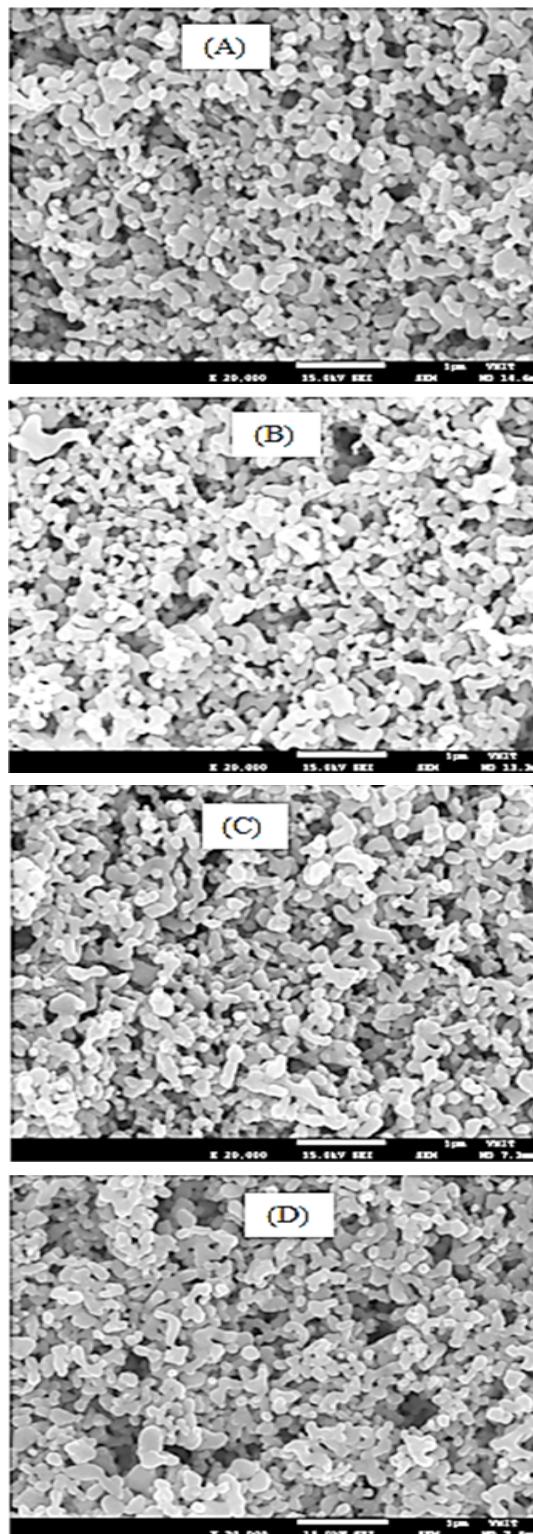

Fig. 1. FE-SEM photographs for (A) SmFeO₃ and Ce-modified SmFeO₃ with dipping time intervals (B) 1 min, (C) 3 min, & (D) 5 minute

All the images appear to be composed of large numbers of grains concluding the porous nature of the film. The agglomeration of few particles was also observed in Fig. 1(A). The size of $SmFeO_3$ grains ranges from 53 nm to 131 nm. The FE-SEM images for Ce surface modified $SmFeO_3$ thick films seem to be comparatively more porous. Therefore these films favor the adsorption and desorption processes in gas sensing mechanism. Ce particles might be deposited at the inner walls of basic $SmFeO_3$ structure and the formation of Ce particles on the surface of $SmFeO_3$ can be confirmed from the EDS micrographs. Moreover, the number of small Ce particles increases with increasing dipping time. The grain size was observed to be ranges from 55

nm to 69 nm in micrograph depicted in Figure 1(D).

Quantitative Elemental Analysis

Figure 2 presents the EDS spectra of pure and Ce-modified $SmFeO_3$ which shows that Ce was deposited on surface modified $SmFeO_3$ films along with Sm, Fe, and O. Moreover, no other impurities were detected in EDS images of as synthesized thick films thereby indicating purity of samples.

Chemical composition in pure and modified $SmFeO_3$ is displaced in Table 1. It is observed that wt % of Ce increased with dipping time. In Ce modified samples, Ce molecules appear to substitute both Sm and Fe molecules.
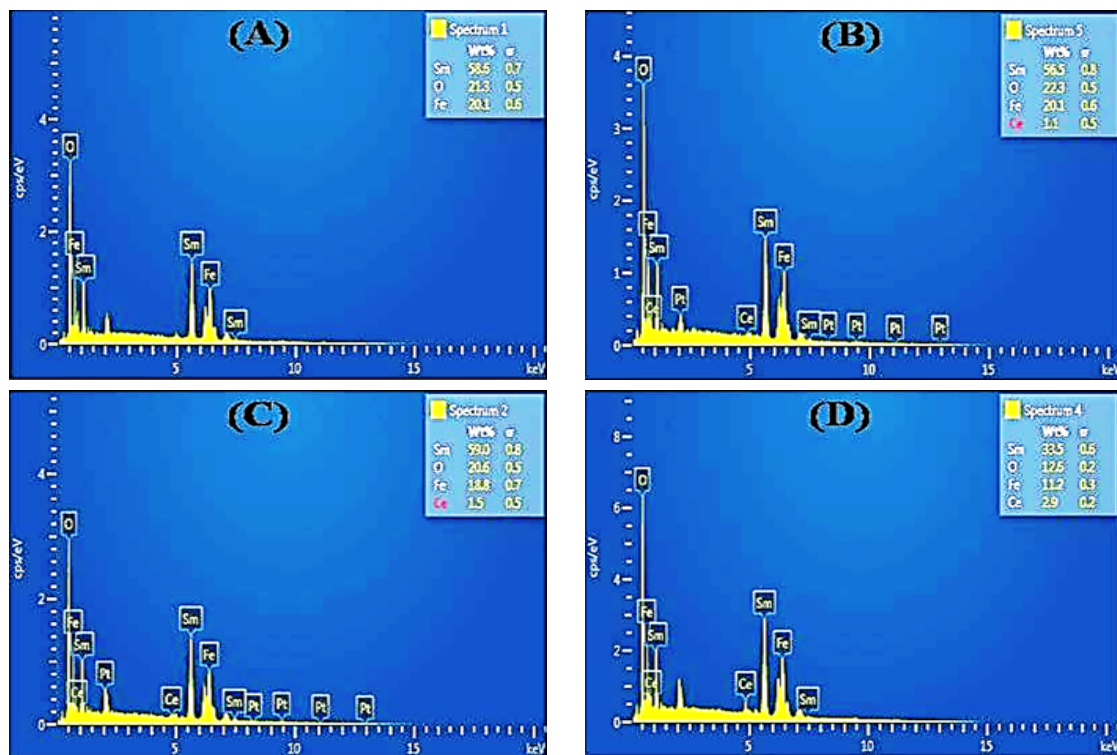

Fig. 2. EDS images for (A) $SmFeO_3$ and Ce-modified $SmFeO_3$ with dipping time intervals (B) 1 min, (C) 3 min, & (D) 5 minute

Table 1: Chemical compositions of pure and Ce-modified $SmFeO_3$ thick films

Samples	Sm (wt%)	O (wt%)	Fe (wt%)	Ce (wt%)
Pure $SmFeO_3$	58.6	21.3	20.1	0
Modified $SmFeO_3$				
Dipping time-1 min	56.5	22.3	20.1	1.1
Dipping time-3 min	59	20.6	18.8	1.5
Dipping time-5 min	53.3	12.6	11.2	2.9

Gas Sensing Performance

Response of pure $SmFeO_3$ film was observed towards different target gases at 100°C and the results indicate that pure $SmFeO_3$ film

was sensitive to ethanol. To investigate the impact of Ce surface modification, gas response of pure and Ce surface modified $SmFeO_3$ films towards 60 ppm ethanol gas was measured by changing the operating temperature from 32⁰C to 400⁰C. Pure $SmFeO_3$ thick film showed extremely small response (S=2.07) towards 60 ppm ethanol gas at 300⁰C. On the other hand, Ce-modified $SmFeO_3$ thick films exhibited improved response and good selectivity for ethanol gas. The change in ethanol gas response according to the operating temperature and gas concentration was investigated for pure and Ce modified $SmFeO_3$ thick films.

Gas Response and Operating Temperature
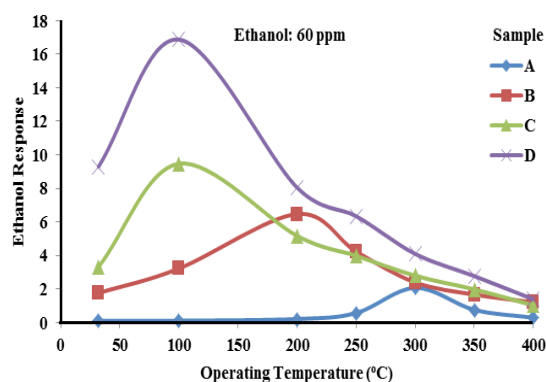Figure 3 shows ethanol gas response at different operating temperatures for all the four samples.

Fig. 3. Gas response for (A) $SmFeO_3$ and Ce-modified $SmFeO_3$ with dipping time intervals (B) 1 min, (C) 3 min, & (D) 5 min towards 60 ppm ethanol

For all the samples, the maximum ethanol gas response was recorded at particular operating temperature below and above which gas response decreased. Maximum response was 6.47 to 60 ppm ethanol for Ce modified $SmFeO_3$ film (dipping time 1 min) and it was observed at 200⁰C. For Ce modified $SmFeO_3$ films with dipping times 3 min and 5 min, same optimal operating temperature was recorded as 100⁰C. But, an improved response (S=16.87) was observed when dipping time was 5 minute.

The gas response of $SmFeO_3$ is due to the resistance change that happens in the adsorption and desorption[17-19]. On the oxide surface, adsorption and desorption of ethanol molecules takes place simultaneously. When operating temperature was increase, more and more ethanol molecules were adsorbed and the sensor responses. However, when

the temperature exceeds the optimum temperature, adsorption becomes slower than desorption and the redox reaction becomes less intense. Hence decrease in gas response is observed at high temperatures. Generally, resistance of $SmFeO_3$ is affected by doping at Sm or Fe site because of the formation of oxygen vacancies. In Ce-modified $SmFeO_3$ thick film, Ce occupies Sm or Fe or both sites which result in the formation of oxygen vacancies. This promotes oxygen adsorption.

Thus, Ce-modified $SmFeO_3$ film with dipping time interval of 3 min exhibited excellent gas response to 60 ppm ethanol at 100⁰C.

Gas Response and Gas Concentration
Figure 4 indicates the values of gas response at different ethanol gas concentration for Ce modified $SmFeO_3$ sensor (dipping time 5 min) at 100⁰C.
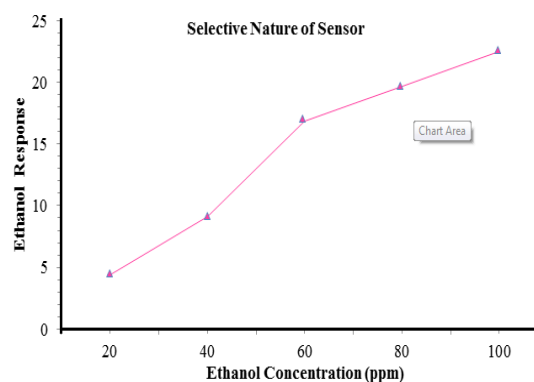

Fig. 4. Gas response for Ce-modified $SmFeO_3$ (dipping time 5 min) for different concentrations of ethanol gas at 100⁰C

The increase in response, but in a different extent, with increasing ethanol gas concentration was observed. Below 20 ppm, the sensor is almost insensitive to ethanol. This low concentration region known as a cut off region indicates that only few ethanol gas molecules reacts with oxygen species. Hence sensor is almost insensitive to ethanol gas. Good linearity between gas response and ethanol concentration was obtained above 60 ppm because ethanol gas molecules reacting with chemisorbed oxygen species are optimum.

Selectivity of Ce-modified $SmFeO_3$ Thick Film
Figure 5 illustrated the bar diagram indicating responses of Ce-modified $SmFeO_3$ thick film at 100⁰C towards LPG, NH_3, CO_2, H_2, C_2H_5OH, Cl_2, and H_2S gas. It is clear from the bar diagram that Ce-modified $SmFeO_3$ thick film sensor (dipping time 5 min) was selective to C_2H_5OH gas against

LPG, NH_3, CO_2, H_2, Cl_2, and H_2S gases. This high selectivity to C_2H_5OH gas was attributed to Ce-modification of $SmFeO_3$ thick film. Distribution of Ce particles for 5 min doping favors the adsorption of ethanol molecules as compared to other gases.
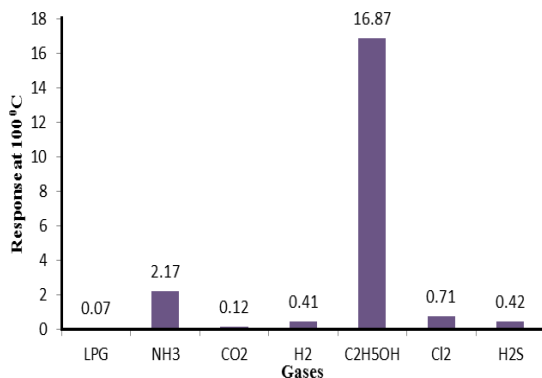

Fig. 5. Selectivity of Ce-modified SmFeO₃ thick film (dipping time 5 min) at 100⁰C

Response-Recovery Profile of the Sensor

Response time is the time taken by sensor to reach 90% of maximum response and recovery time is time taken by sensor to fall to 90% of maximum response. Response-recovery profile for Ce-modified $SmFeO_3$ thick film (dipping time 5 min) to 60 ppm ethanol at 100⁰C was depicted in Fig. 6. Response and recovery times recorded for as prepared Ce-modified $SmFeO_3$ thick film (dipping time 5 min) sensor were approximately 24 sec and 34 sec respectively.
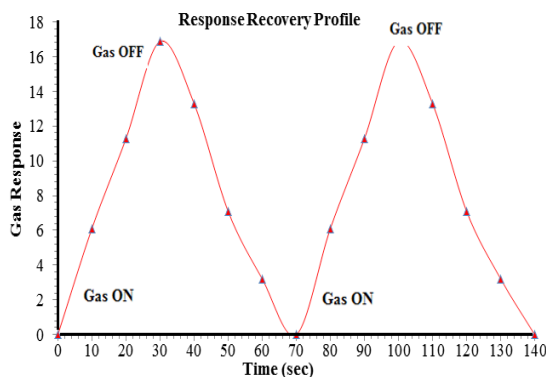

Fig. 6. Response-recovery profiles of Ce-modified SmFeO₃ sensor (dipping time 5 min) towards 60 ppm ethanol at 100⁰C

Stability of Sensor

The gas response of Ce-modified $SmFeO_3$ (dipping time 5 min) sensor to 60 ppm ethanol at 100⁰C was observed for the period of 90 days. Results depicted in Fig. 7 indicate good stability and durability for Ce-modified $SmFeO_3$ (dipping time 5 min) sensor towards ethanol.
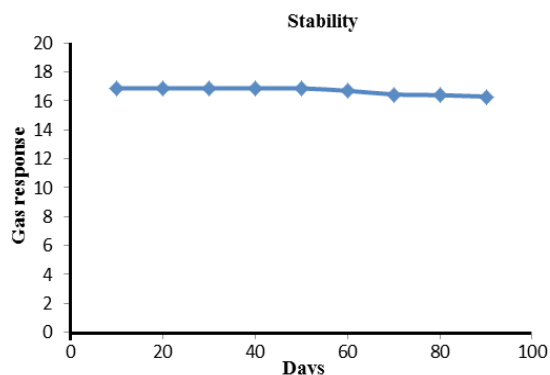

Fig. 7. Stability of Ce-modified SmFeO₃ sensor (dipping time 5 min) towards 60 ppm ethanol at 100⁰C

Ethanol Gas-Sensing Mechanism

Ethanol sensing is based on the resistance change in presence of air and then in presence of ethanol. The change in resistance depends on amount of adsorbed oxygen species on the surface of sensor and the ethanol gas species interacting with chemisorbed oxygen species. Being a p-type semiconductor, holes are the charge carriers in $SmFeO_3$. In presence of air, there is adsorption of oxygen molecules and these adsorbed oxygen trap the electrons from the metal to form highly reactive ionic species like O_2^-, O^- and O^{2-}. The formation of oxygen species depends on temperature and expressed as follows.[25]

$$O_{2(air)} \xrightarrow{upto\ 150^0C} O_2^- \xrightarrow{upto\ 450^0C} 2O^- \xrightarrow{above\ 450^0C} O^{2-}$$
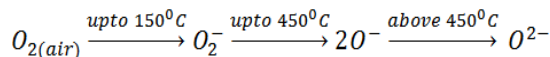
Because of this chemisorption of oxygen molecules, concentration of holes increases. Therefore, hole accumulation layer is formed near the oxide surface and it act as potential barrier between neighboring grains. As a result, sensor has small resistance in presence of air. When such sensor gets contact with ethanol, catalytic oxidation of ethanol takes place producing CO_2 and H_2O. The reaction occurs as follows[26].

$$CH_3\ CH_2\ OH + 6O^- \rightarrow 2CO_2 + 3H_2O + 6e^-$$
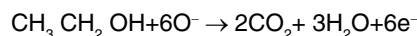
During this desorption process, trapped electrons are returned back and the width of accumulation layer decreases. Thus there is increase in sensor resistance in presence of ethanol. The difference between these two resistances produces gas response.

Thus the present work reveals that pure $SmFeO_3$ thick film fabricated by the screen printing

technique, exhibited selective response to ethanol than other tested target gases. All Ce-surface modified $SmFeO_3$ thick films showed improved response to ethanol. Among these Ce-modified $SmFeO_3$ thick films, the sample with dipping time interval of 5 min exhibited excellent ethanol sensing properties such as, maximum response (16.87 at 100^0C), response time (24 sec), recovery time (34 sec), excellent stability, and good selectivity towards ethanol. Thus Ce-modified $SmFeO_3$ can be a potential material in the fabrication of ethanol sensor. Dipping technique can be used for the surface modification of $SmFeO_3$ thick film.

Conflict of Interest
The author(s) declare no conflict of interest.

REFERENCES

1. Gautam, Y. K.; Sharma K.; Tyagi, S.; Ambedkar, A. K.; Chaudhary, M.; Singh, P., *J. Roy. Soc. Open Sci.*, **2021**, *8*, 201324. https://doi.org/10.1098/rsos.201324.
2. Zhang, C.; Luo, Y.; Luo, J.; Xu, M. D. Sens., *Actuators A Phys.*, **2019**, *289*, 118-133. https://doi.org/10.1016/j.sna.2019.02.027.
3. Agrawal, S.; Rai, P.; Gatel, E.; Guell, F.; Kumar, M.; Awasthi, K. *Sens. Actuator B Chem.*, **2019**, *292*, 24-31. https://doi.org/10.1016/j.snb.2019.04.083.
4. Tian, X.; Cui, X.; Lai, T.; Ren, J.; Yang, Z.; Xiao, M.; Wang, Y., *Nano Mater. Sci.*, **2021**, *3*, 390-403. https://doi.org/10.1016/j.nanoms.2021.05.011.
5. Han, M. A.; Kim, H. J.; Lee, H. C.; Park, J. S.; Lee, H. N., *Appl. Surf. Sci.*, **2019**, *481*, 133-137. https://doi.org/10.1016/j.apsusc.2019.03.043.
6. Liu, C.; Lu, H.; Zhang, J.; Zhu, G.; Yang, Z.; Yin, F.; Wang, C., *Sens. Actuator B Chem.*, **2018**, *263*, 557-567.
7. Dong, C.; Zhao, R.; Yao, L.; Ran, Y.; Zhang, X.; Wang, Y., *J. Alloys and Comp.*, **2020**, *820*, 153194. https://doi.org/10.1016/j.jallcom. 2019.153194.
8. Praveena, K.; Bharathi, P.; Liu, H. L.; Varma, K. B., *Ceram. Int.*, **2016**, *42*, 13572-13585.
9. Huang, H. T.; Zhang, W. L.; Zhang, X. D.; Guo, X., *Sens. Actuator B Chem.*, **2018**, *265*, 443-451. https://doi.org/10.1016/j.snb.2018.03.073.
10. Fan, W.; Sun, Z.; Wang, J.; Zhou, J.; Wu, K. *J. Power Sources.*, **2016**, *312*, 223-233.
11. Zhang, Y.; Zou, H.; Peng, J.; Duan, Z.; Ma, M.; Xin, X.; Zheng, X. *Sens. Actuator B Chem.*, **2018**, *272*, 459-467. https://doi.org/10.1016/j.snb.2018.06.007.
12. Bukhari, S. M.; Giorgi., *J. B. Solid State Ion.*, **2010**, *181*, 392–401. https://doi.org/10.1016/j.ssi.2010.01.017.
13. Bukhari, S. M.; Giorgi, J. B. *Solid State Ionics.*, **2009**, *180*, 198–204. https://doi.org/10.1016/j.ssi.2008.12.002.
14. Hao, P.; Qu, G. M.; Song, P.; Yang, Z. X.; Wang, Q., *Rare Mater.*, **2021**, *40*, 1651–1661 https://doi.org/10.1007/s12598-020-01672-2.
15. Xue, Z.; Cheng, Z.; Xu, J.; Xiang, Q.; Wang, X.; Xu., *J. ACS. Appl. Mater. Int.*, **2017**, *9*, 41559-41567. https://doi.org/10.1021/acsami.7b13370.
16. Pargoletti, E.; Cappelletti, G., *Nanomaterials.*, **2020**, *10*, 1485. https://doi.org/10.3390/nano10081485.
17. Fang, S.; Peng, H.; Zhao, M.; Hu, J.; Chen, L., *J. Fun. Mater.*, **2017**, *28*, 54–60.
18. Niu, X.; Du, W.; Jiang, K. *J. Trans. Tech.*, **2013**, *22*, 5–7.
19. Zhao, M.; Peng, H.; Hu, J.; Han, Z., *Sens. Actuator B Chem.*, **2008**, *129*, 953–957. https://doi.org/10.1016/j.snb.2007.10.012.
20. Mankar, R. B.; Kapse, V. D.; Patil, D. R., *Asian Journal of Chemistry.*, **2023**, *35*, 1485-1490. https://doi.org/10.14233/ajchem.2023.27874
21. Shinde, S. D.; Gaikwad, V.B.; Patil, G.E.; Kajale, D.D.; Jain, G.H., *Int. J. Nano.*, **2012**, 5, 126-135. https://doi.org/10.1504/IJNP.2012.046239.
22. Maity, R.; Sakhya, A.; Dutta, A.; Sinha,T. P., *Mater. Chem. and Phys.*, **2019**, *223*, 78-87. https://doi.org/10.1016/j.matchemphys.2018.10.038.
23. Patil, R.P.; Gaikwad,V. B.; Jain, G.H.; Gaikwad, S. S., *Int. J. of Chem. and Phys Sci.*, **2018**, *7*, 259-267.
24. Nahire, S.B.; Patil, G.E.; Jain, G.H.; Gaikwad, V.B.; Deshmukh, S.B., *Int. J. Res. in Applied Science & Engineering Technology.*, **2017**, *9*, 2535-2543.
25. Patil, S. D.; Nikam,H. A.; Sharma, Y.C.; Yadav, R. S. Kumar, D.; Singh, A. K.; Patil D.R., *Sens. Actuator B Chem.*, **2023**, *377*, 1-10. https://doi.org/10.1016/j.snb.2022.133080.
26. Xiang, J.; Chen, X.; Zhang, X.; Gong, L.; Zhang, Y.; Zhang, K., *Mater. Chem. Phys.*, **2018**, *213*, 122–129. https://doi.org/10.1016/j.matchemphys.2018.04.024.